

RESEARCH ARTICLE

10.1002/2015WR017413

Bayesian-information-gap decision theory with an application to CO₂ sequestration

D. O'Malley¹ and V. V. Vesselinov¹

¹Computational Earth Science Group, Earth and Environmental Sciences Division, Los Alamos National Laboratory, Los Alamos, New Mexico, USA

Key Points:

- We develop a decision framework for subsurface flow and transport applications
- Probabilistic and information-gap methods are combined for uncertainty quantification
- An decision-support scenario for geologic carbon sequestration is considered

Correspondence to:

D. O'Malley,
omalled@lanl.gov

Citation:

O'Malley, D., and V. V. Vesselinov (2015), Bayesian-information-gap decision theory with an application to CO₂ sequestration, *Water Resour. Res.*, 51, doi:10.1002/2015WR017413.

Received 17 APR 2015

Accepted 26 JUL 2015

Accepted article online 30 JUL 2015

Abstract Decisions related to subsurface engineering problems such as groundwater management, fossil fuel production, and geologic carbon sequestration are frequently challenging because of an over-abundance of uncertainties (related to conceptualizations, parameters, observations, etc.). Because of the importance of these problems to agriculture, energy, and the climate (respectively), good decisions that are scientifically defensible must be made despite the uncertainties. We describe a general approach to making decisions for challenging problems such as these in the presence of severe uncertainties that combines probabilistic and nonprobabilistic methods. The approach uses Bayesian sampling to assess parametric uncertainty and Information-Gap Decision Theory (IGDT) to address model inadequacy. The combined approach also resolves an issue that frequently arises when applying Bayesian methods to real-world engineering problems related to the enumeration of possible outcomes. In the case of zero nonprobabilistic uncertainty, the method reduces to a Bayesian method. To illustrate the approach, we apply it to a site-selection decision for geologic CO₂ sequestration.

1. Introduction

A decision is the end-goal of many scientific efforts. Uncertainty often plays an important role in these decisions. The presence of uncertainty is especially pronounced in earth science applications where models are often inadequate (due to, e.g., geologic heterogeneity) and the decision may have enormous consequences (e.g., deployment of CO₂ sequestration to address climate change). Hence, there is a need for robust methodologies and techniques to support decisions in earth science applications.

The standard approach to scientific decision support is for a scientist or group of scientists to analyze data and utilize models to quantify an uncertain outcome. The quantification of the uncertain outcome can then be presented to a decision maker (e.g., a manager, government agency, or policy-maker) whereafter a decision is made. One potential difficulty with this approach is that uncertainty quantification is a complicated subject and the decision maker may not fully understand the impact of the uncertainty on the decision [Liu *et al.*, 2008].

One way to mitigate this difficulty is by explicitly incorporating the decision goals within the uncertainty quantification framework [Berger, 1985; Ben-Haim, 2006]. This places more of the burden of understanding the impact of the uncertainty on the decision with the scientists who are quantifying the uncertainty, and less of burden with the decision maker. We explore one such approach that combines Bayesian methods for probabilistic uncertainty quantification [Lee, 2012] with a nonprobabilistic approach called Information-Gap Decision Theory (IGDT) [Ben-Haim, 2006]. IGDT is considered a nonprobabilistic approach, because it does not include a notion of likelihood. Instead, it describes a set of possibilities (without assigning probabilities) that are within a given "horizon of uncertainty." The horizon of uncertainty can range from zero (where the set of possibilities contains only one element—the nominal element) to infinity, with the set of possibilities increasing as the horizon of uncertainty increases. The horizon of uncertainty is essentially an index to nested sets of possibilities. The horizon of uncertainty can also be called "level of information-gap uncertainty." For other examples of applying IGDT in a hydrogeological context, see Harp and Vesselinov [2013] and O'Malley and Vesselinov [2014a].

The Bayesian approach provides a mathematically rigorous method for quantifying parametric uncertainty. IGDT makes it possible to incorporate decision goals and provides a mechanism to make the Bayesian

analysis more scientifically rigorous (as opposed to mathematically rigorous). We explore this approach in a general context in section 2. While the approach is general enough to be applied to a wide set of problems, we explicitly apply it in the context of a geologic CO₂ sequestration decision scenario in section 3.

Geologic CO₂ sequestration is an important technology for mitigating climate change due to rising levels of CO₂ in the atmosphere. In a well-chosen reservoir, it is likely 99% of geologically sequestered carbon would remain sequestered for over 1000 years [Metz *et al.*, 2005]. The key here is that the reservoir be well-chosen so as to avoid leakage through wells, faults, and fractures. There is also the potential to “trigger small seismic events” [Metz *et al.*, 2005]. Therefore, a reservoir should be chosen so that the injected CO₂ has little potential to seismic activity. The decision scenario that we explore is to choose a reservoir for CO₂ injection that avoids leakage and induced seismicity.

There were several studies on the analysis and model simulation (analytical, semianalytical, and numerical) of CO₂ leakage [Pruess, 2004; Doughty and Pruess, 2004; Nogues *et al.*, 2011; Zhou *et al.*, 2009; Gasda *et al.*, 2004; Avci, 1994; Nordbotten *et al.*, 2004, 2005; Cihan *et al.*, 2011]. Fewer studies were performed on model estimation of the leakage based on inverse analyses of observed pressure changes in the subsurface (using synthetic or field data). The permeability values of actual abandoned wells were estimated through inverse analysis of observed data in the field in Gasda *et al.* [2011]. The feasibility of leakage pathway detection was explored using inverse modeling-based pressure changes induced by a leaky well measured from monitoring wells in Jung *et al.* [2012]. The use of synthetic pressure and surface-deformation measurements was tested for the detection of leakage pathways in Jung *et al.* [2013]. A comparison of several sensitivity analyses was carried out in the context of CO₂ sequestration in Wainwright *et al.* [2014]. A comprehensive system-level model for performance assessment of geologic CO₂ sequestration that addresses uncertainty probabilistically was described in Stauffer *et al.* [2006, 2008]. Our approach builds upon this work by utilizing existing modeling tools and probabilistic uncertainty quantification methods, but combining them with IGDT.

2. Bayesian-Information-Gap Decision Theory

Three forms of uncertainty are addressed within the Bayesian-Information-Gap Decision Theory (BIG DT) framework: forward model uncertainty/inadequacy (including model structural uncertainty), model parameter uncertainty, and uncertainty in the distribution of residuals representing mismatches between field observations and model predictions (this type of uncertainty typically arises in inverse model analyses where field observations are used to calibrate a model and estimate unknown model parameters). The approach we describe here generalizes a previous application of this approach to a groundwater contaminant remediation problem [O'Malley and Vesselinov, 2014b].

2.1. Model Inadequacy

It is necessary to address model inadequacy because models (including the model we employ here) almost always oversimplify the physics associated with the actual processes. For example, uniform parameters are sometimes used to characterize aquifer properties. In reality these parameters are likely to be heterogeneous, and this will impact the model predictions. When models include aquifer heterogeneity, the scale of the model heterogeneity is often much coarser than the scale of the aquifer heterogeneity [e.g., Wen and Gómez-Hernández, 1996]. Another example is related to deformation process associated with fluid pressure changes in aquifers [Wang and Kümpel, 2003]. Frequently, these processes are ignored in the models as well.

To begin, we assume that there is a parametric physics model that makes predictions. We also assume that the model has unknown parameters that can be estimated by model calibration against site observations. We then utilize this parametric model to inform a decision. Denote this parametric model by

$$\mathbf{F}(\mathbf{q})=[F_1(\mathbf{q}), F_2(\mathbf{q}), \dots, F_N(\mathbf{q})], \quad (1)$$

where \mathbf{q} is the model parameters (model inputs) and the F_i is the model outputs. For example, in the geologic CO₂ sequestration problem studied here, the components of \mathbf{q} are aquifer properties, well properties, and an injection rate, and the F_i is water levels at different times and locations.

We address model inadequacy using an information-gap model of uncertainty, $M(\epsilon, \mathbf{q})$, where ϵ is called the horizon (or level) of uncertainty. For each $\epsilon \geq 0$, $M(\epsilon, \mathbf{q})$ is the set of model outputs that are possible

within a given horizon of uncertainty. These sets should be chosen so as to represent the uncertainties as well as possible (an art more than a science) and must have the following two properties. First, when $\epsilon = 0$, $M(\epsilon, \mathbf{q})$ is the set containing only the element $\mathbf{F}(\mathbf{q})$, that is,

$$M(0, \mathbf{q}) = \{\mathbf{F}(\mathbf{q})\}. \quad (2)$$

This ensures that the parametric model predictions are the first thing that should be considered and nothing else should be considered when the horizon of uncertainty is equal to zero. Second, the sets must be increasing with ϵ , that is, when $\epsilon_1 \leq \epsilon_2$

$$M(\epsilon_1, \mathbf{q}) \subseteq M(\epsilon_2, \mathbf{q}). \quad (3)$$

This ensures that as the horizon of uncertainty increases, the set of possible model outputs should only get bigger, never getting smaller (i.e., the sets are nested).

2.2. Parametric Uncertainty

Generally the most appropriate parameter values, \mathbf{q} , to be used in the parametric model, $\mathbf{F}(\mathbf{q})$, are unknown. We employ Bayes theorem to produce a posterior probability distribution for the parameters, conditioning on a vector of observations, \mathbf{O} . Bayes theorem provides a systematic way for updating the posterior distribution of the parameters based on observed data. Formally, this is expressed as

$$f(\mathbf{q}|\mathbf{O}) = \frac{f(\mathbf{O}|\mathbf{q})f(\mathbf{q})}{\int_{\Omega} f(\mathbf{O}|\mathbf{q})f(\mathbf{q})d\mathbf{q}}, \quad (4)$$

where $f(\mathbf{q}|\mathbf{O})$ is the posterior probability density function for the parameters conditioned on the observations, $f(\mathbf{O}|\mathbf{q})$ is the probability density function for the observations conditioned on the parameters, and $f(\mathbf{q})$ is the prior probability density function for the parameters. Equation (4) is related to the parametric model through $f(\mathbf{O}|\mathbf{q})$ which typically takes the form

$$f(\mathbf{O}|\mathbf{q}) = g(O_1 - F_{i_1}(\mathbf{q}), O_2 - F_{i_2}(\mathbf{q}), \dots, O_M - F_{i_M}(\mathbf{q})), \quad (5)$$

where g is some multivariate probability density function, F_{i_j} is a model output that corresponds to observation O_{j_i} , and the $O_{j_i} - F_{i_j}(\mathbf{q})$ are called residuals. For example, if the residuals follow a multivariate normal distribution with mean μ and covariance Σ , then

$$g(\mathbf{x}) = \frac{\exp\left[-(\mathbf{x} - \mu)^T \Sigma^{-1} (\mathbf{x} - \mu) / 2\right]}{\sqrt{(2\pi)^M |\Sigma|}}. \quad (6)$$

Each set, $M(\epsilon, \mathbf{q})$, has a probability density associated with it. This probability density is given by equation (4). In the same way that we might represent a random variable for the parameters with a capital \mathbf{Q} , we will use $M(\epsilon, \mathbf{Q})$ to represent a random set.

In practice, equation (4) is frequently difficult to compute, because the integral in the denominator must often be taken over a high-dimensional space. This difficulty can be circumvented by employing Markov Chain Monte Carlo (MCMC) sampling methods that require only ratios, $f(\mathbf{q}_1|\mathbf{O})/f(\mathbf{q}_2|\mathbf{O})$, which eliminate the dependence on the constant denominator [Metropolis et al., 1953; Gelfand and Smith, 1990; Geyer, 1992]. A number of techniques [e.g., Plummer, 2003; Vrugt et al., 2009; Lunn et al., 2009; Goodman and Weare, 2010; Vihola, 2012] have been developed to perform this sampling effectively and efficiently. In the application considered, we have elected to use the sampler described in Vihola [2012] due to its robustness and ease of use.

2.2.1. Uncertainty in the Residual Distribution

In the presented analysis, model inversion is applied where field observations are used to calibrate the model and estimate the unknown model parameters. However, the results of the inverse analysis strongly depend on assumptions that are made about the statistical properties of the residuals $f(\mathbf{O}|\mathbf{q})$. In complex applications, the correct form for $f(\mathbf{O}|\mathbf{q})$ is usually, perhaps always, uncertain. This uncertainty implies that any expected values or probabilities that result from applying equation (4) are also uncertain. It is common practice to choose $f(\mathbf{O}|\mathbf{q})$ for convenience rather than correctness. For example, it is sometimes assumed that observations are independent, Gaussian, or both without any rigorous justification. It is important to

note that the assumption of a particular residual distribution implies a certain form for the model inadequacy. In this way, the uncertainty in the residual distribution accounts for model inadequacy as well.

To address this uncertainty, we utilize an information-gap uncertainty model. As with the previous information-gap uncertainty model (section 3.1), this is a collection of sets that are parameterized in terms of the horizon of uncertainty, ϵ , and we denote this set $U(\epsilon)$. As before, it must have the property that if $\epsilon_1 \leq \epsilon_2$ then

$$U(\epsilon_1) \subseteq U(\epsilon_2). \quad (7)$$

When $\epsilon = 0$, $U(0)$ must be a set containing only one likelihood function for the observations conditioned on the parameters, \mathbf{q} . This likelihood function is called the nominal likelihood function, and we denote it by $f_0(\mathbf{O}|\mathbf{q})$, so that

$$U(0) = \{f_0(\mathbf{O}|\mathbf{q})\}. \quad (8)$$

In IGDT, the word “nominal” is used in the sense of “stated or expressed but not necessarily corresponding exactly to the real value” [Jewell *et al.*, 2001]. Here the nominal concept is used to define an initial conceptualization of the statistical relationship between the model parameters and the observations. In some sense, this initial set, $U(0)$, defines our best estimate for the statistical relationship, and the information-gap model, $U(\epsilon)$, describes the uncertainty in the estimate.

2.3. Making a Decision

Before making a decision, it is necessary to state some performance requirements or decision goals. In the BIG DT framework, these goals are of two types. The first type is related to the behavior of the physical system, and states the system behavior that we would like to take place. For example, in a groundwater remediation application of this approach [O'Malley and Vesselinov, 2014b], this statement was that the contaminant concentration at a point of compliance should be below a certain threshold. Whether or not this goal is satisfied, which is determined via the model predictions, $\mathbf{F} = [F_1, F_2, \dots, F_N]$, where these models are not necessarily the parametric model described in equation (1), and may be any of the models contained in the sets, $M(\epsilon, \mathbf{q})$. Formally, this can be described with a binary function

$$G(\mathbf{F}) = \begin{cases} 1, & \text{if the outcome is a success} \\ 0, & \text{if the outcome is a failure} \end{cases} \quad (9)$$

The second type is a requirement that the probability of violating the desired system behavior be below a threshold, P_0 . Formally, this takes the form

$$\forall \epsilon \in U(\epsilon), P(\exists \mathbf{F} \in M(\epsilon, \mathbf{Q}) : G(\mathbf{F}) = 0) < P_0, \quad (10)$$

where the probabilities are computed via equation (4). Note that here \forall should be read as “for all,” \exists should be read as “there exists” and $:$ should be read as “such that.” Unrolling this formality, we can say that the notation,

$$\exists \mathbf{F} \in M(\epsilon, \mathbf{Q}) : G(\mathbf{F}) = 0, \quad (11)$$

expresses the idea that within the horizon of uncertainty, ϵ , it is possible ($\exists \mathbf{F} \in M(\epsilon, \mathbf{Q})$) to fail ($G(\mathbf{F}) = 0$). The notation,

$$\forall \epsilon \in U(\epsilon), P(\dots) < P_0, \quad (12)$$

expresses the idea that it is guaranteed ($\forall \epsilon \in U(\epsilon)$) that the probability will be below the threshold, P_0 ($P(\dots) < P_0$). Putting this together, equation (10) states that within the horizon of uncertainty, ϵ , the probability of it being possible to fail is below the threshold, P_0 . In other words, within the horizon of uncertainty, ϵ , it is not possible that the probability of failure exceeds or equals P_0 .

We now define the information-gap robustness for this system as

$$\hat{\epsilon} = \max \{ \epsilon \geq 0 : \forall \epsilon \in U(\epsilon), P(\exists \mathbf{F} \in M(\epsilon, \mathbf{Q}) : G(\mathbf{F}) = 0) < P_0 \}. \quad (13)$$

The information-gap robustness defines the maximum horizon of uncertainty at which the probability of it being possible to fail is below the threshold, P_0 . When making a decision among alternatives, one chooses the option that has the greatest information-gap robustness, $\hat{\epsilon}$. These options might be different remedies in a groundwater contamination scenario [O'Malley and Vesselinov, 2014b] or different geologic sites at which CO_2 could be injected. We will now explore applying this approach to the latter situation.

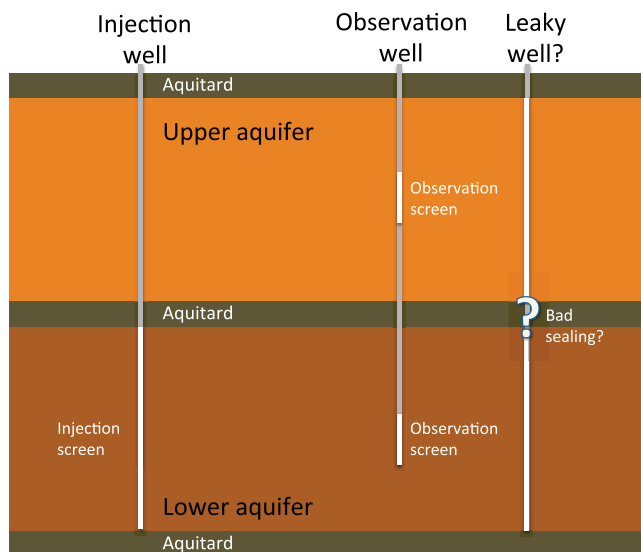


Figure 1. The hydrogeological setup for a CO₂ injection test consisting of two aquifers separated by an aquitard with an injection well, an observation well with two screens, and potentially a nearby leaky well.

3. Application to Geologic CO₂ Sequestration

We now consider an application of the BIG DT decision analysis to a CO₂ sequestration problem. The problem is the selection of a site at which CO₂ will be injected into a deep aquifer. The goals of the decision analysis are to

1. limit the possibility of inducing a high overpressure in the host formation to avoid inducing seismicity and
2. limit the possibility of inducing a high overpressure/flow into the aquifer overlying the host formation to avoid groundwater contamination

The suitability of two similar sites is evaluated. Both sites contain a host aquifer and an overlying aquifer separated by an aquitard that prevents flow and the propagation of pressure

between the two aquifers (see Figure 1). The suitability is evaluated with a 30 day injection test. The pressure response is observed in two screens (one in the host aquifer and the other in the overlying aquifer) of an observation well.

The known parameters at the sites are the injection rate, the conductivities, specific storages, and thicknesses of both the host aquifer and the overlying aquifer. What is unknown is whether there is a leaky well in the area, its location, geometry, and its resistivity to flow. The parameter values for the two sites are given in Table 1. Note that all the parameters are the same except that the leaky well at Site 1 has a lower resistivity than the leaky well at Site 2. More information on the model and the parameters used are presented in section 3.1.

3.1. Physical Model

A number of analytical and semianalytical models have been developed that capture the impact of injection in deep aquifers on shallower aquifers [e.g., Avci, 1994; Nordbotten et al., 2004, 2005; Cihan et al., 2011]. Since the focus here is on the decision analysis and not the model, the relatively simple model developed in Avci [1994] is employed. We note, however, that more complex models that involve more aquifer layers or more wells could be employed with the methodology developed here. This solution for the flow through

Parameter	Description	Site 1
Q_w	Injection rate	0.01 (m ³ /s)
K_1	Upper aquifer conductivity	10 ⁻⁴ (m/s)
K_2	Lower aquifer conductivity	10 ⁻⁶ (m/s)
L_1	Upper aquifer thickness	100 (m)
L_2	Lower aquifer thickness	200 (m)
S_{c1}	Upper aquifer specific storage	7 × 10 ⁻⁵ (m ⁻¹)
S_{c2}	Lower aquifer specific storage	10 ⁻⁵ (m ⁻¹)
r_a	Leaky well radius	0.1 (m)
Ω	Leaky well resistivity	Site 1: 3 × 10 ³ (s/m ²), Site 2: 10 ⁴ (s/m ²)
r_1	Distance from leaky well to upper obs. screen	100 (m)
r_2	Distance from leaky well to lower obs. screen	100 (m)
r_w	Distance from injection well to lower obs. screen	25 (m)
R	Distance from injection well to leaky well	93.75 (m)
Δh	Head difference between upper and lower aquifer	0 (m)

the leaky well and the hydraulic head buildup at each observation screen can be expressed concisely in Laplace space

$$\tilde{Q}_c = \frac{\frac{Q_w}{2\pi K_2 L_2} K_0 \left(R \sqrt{\omega S_{c2}/K_2} \right) + \Delta h}{\omega \left[\Omega + \frac{1}{2\pi K_2 L_2} K_0 \left(r_a \sqrt{\omega S_{c2}/K_2} \right) + \frac{1}{2\pi K_1 L_1} K_0 \left(r_a \sqrt{\omega S_{c1}/K_1} \right) \right]}, \quad (14)$$

$$\tilde{S}_1 = \frac{\tilde{Q}_c}{2\pi K_1 L_1} K_0 \left(r_1 \sqrt{\omega S_{c1}/K_1} \right), \quad (15)$$

$$\tilde{S}_2 = \frac{Q_w}{2\pi K_2 L_2 \omega} K_0 \left(r_w \sqrt{\omega S_{c2}/K_2} \right) - \frac{\tilde{Q}_c}{2\pi K_2 L_2} K_0 \left(r_2 \sqrt{\omega S_{c2}/K_2} \right), \quad (16)$$

where Q_c is the flow through the leaky well; K_0 is the modified Bessel function of the second kind and zero order; S_1 and S_2 are the hydraulic head buildup in the upper and lower aquifers, respectively; Q_w is the injection rate; K_1 and K_2 are the conductivities in the upper and lower aquifers, respectively; L_1 and L_2 are the thicknesses of the upper and lower aquifers, respectively; S_{c1} and S_{c2} are the specific storage coefficients of the upper and lower aquifers, respectively; r_a is the radius of the leaky well; Ω is the resistivity within the leaky well, r_1 and r_2 are the distances from the leaky well to the observation screens in the upper and lower aquifers, respectively, r_w is the distance from the injection well to the observation screen in the lower aquifer; R is the distance from the injection well to the leaky well; Δh is the preexisting hydraulic head difference between the upper and lower aquifers; and ω is the Laplace variable. Following the numerical approach used in *Cihan et al.* [2011] for a more general solution, the solution is inverted from Laplace space numerically using Stehfest inversion [Stehfest, 1970a, 1970b]. In the notation of section 2, the F_i from equation (1) is

$$F_i(\mathbf{q}) = S_1(t_i; \mathbf{q}), i = 1, 2, \dots, 30, \quad (17)$$

$$F_i(\mathbf{q}) = S_2(t_{i-30}; \mathbf{q}), i = 31, 32, \dots, 60, \quad (18)$$

where $t_i = 24i$ [h] and \mathbf{q} is a vector of uncertain parameters

$$\mathbf{q} = [r_a, R, \Omega, r_1] \quad (19)$$

and the remaining parameters are known (Table 1). Note that because the observation screens in the upper and lower aquifer are part of the same well in this scenario, $r_1 \equiv r_2$.

The model is used to compute the synthetic pressure build-up resulting from the injection test. Due to a variety of factors including barometric effects, nearby pumping or injection not included in the model, earth tide effects, and/or seismic activity, the signal recorded at the observation screens would contain a noisy representation of the signal from the injection test. Therefore, the synthetic pressure build-up signal was combined with a random noise to produce a set of daily "observations" over a simulated 30 day injection test (see Figure 2).

The random noise signal is a fractional Gaussian noise [Mandelbrot and Van Ness, 1968] with a Hurst exponent, $H = 3/4$, and standard deviation, $\sigma = 2.5$ (cm). This is a zero-mean Gaussian process with covariance given by

$$E[G_H(t)G_H(s)] = \frac{\sigma^2}{2} (|t+1-s|^{2H} - 2|t-s|^{2H} + |t-1-s|^{2H}), \quad (20)$$

where G_H is a fractional Gaussian noise. Note that the G_H here is unrelated to the G from equation (9). With $H > 1/2$, the noise exhibits persistent behavior—if the signal is positive at one time, it is more likely to be positive at a future time than it is to be negative. With $H < 1/2$, the noise exhibits antipersistent behavior—if the signal is positive at one time, it is more likely to be negative at a future time than it is to be positive. When $H = 1/2$, the noise is a Gaussian white noise which exhibits neither persistence nor antipersistence. Gaussian white noise is expected if the residuals are unbiased, independent, and normally distributed.

Fractional Gaussian noise was chosen somewhat arbitrarily. Other forms of noise could have been used as well. Here we have chosen a value of H in the middle of the persistent regime, because experience indicates

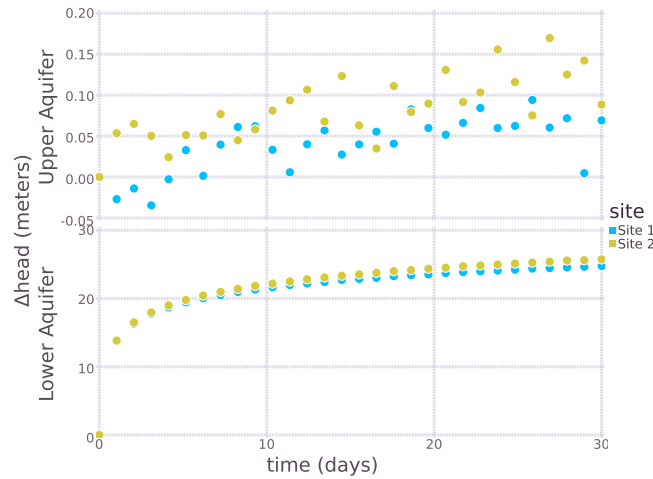


Figure 2. The set of synthetic observations generated by combining the physical model using the true parameters with a random noise that are analyzed in the Bayesian component of the uncertainty quantification.

that residuals tend to be persistent. The noise level again was chosen to be in line with our experience examining residuals, but will depend on how accurately the model reflects the activity in the aquifers. For example, if there is a strong pumping signal that is not included in the model, the noise level will likely be much higher.

3.2. Model Inadequacy

The model described in section 3.1 captures the most vital physics of the scenario described, but certainly not all of the physics. For example, the model assumes that the aquifers are homogeneous, isotropic, extend infinitely, and are separated by a totally impermeable layer. We employ an information-gap

uncertainty model to deal with these issues of inadequacy in the physical model

$$M(\epsilon, \mathbf{q}) = \left\{ \mathbf{F} : \left| \frac{F_i - F_i(\mathbf{q})}{F_i(\mathbf{q})} \right| \leq \epsilon, \forall i \right\}. \quad (21)$$

The set $M(\epsilon, \mathbf{q})$ represents a set of possibilities, in this case changes in head, that are decreasingly close (with increasing ϵ) to the model prediction, $F(\mathbf{q})$. This is necessary, because our model may not be able to represent the response of the head in the aquifer to the injection. The sets $M(\epsilon, \mathbf{q})$ represent the possibilities within the horizon of uncertainty, ϵ . The use of this information-gap uncertainty model essentially states that the set of possible models at the horizon of uncertainty, ϵ , is the set of models with a relative difference from the parametric model less or equal to than ϵ .

Note that $M(0, \mathbf{q}) = \{F(\mathbf{q})\}$, satisfying equation (2). Also, if $\epsilon_1 \leq \epsilon_2$ and $\mathbf{F} \in M(\epsilon_1, \mathbf{q})$ then

$$\left| \frac{F_i - F_i(\mathbf{q})}{F_i(\mathbf{q})} \right| \leq \epsilon_1 \leq \epsilon_2, \forall i. \quad (22)$$

This implies that $\mathbf{F} \in M(\epsilon_2, \mathbf{q})$, and hence $M(\epsilon_1, \mathbf{q}) \subseteq M(\epsilon_2, \mathbf{q})$ as required by equation (3). Therefore, the sets $M(\epsilon, \mathbf{q})$ forms a valid information-gap uncertainty model.

3.3. Parametric Uncertainty

Parametric uncertainty is handled using the approach described in section 2.2. The prior distribution is

$$f(\mathbf{q}) \equiv f(r_a, R, \Omega, r_1) \propto \begin{cases} f_{r_a}(r_a) f_R(R) f_\Omega(\Omega) f_{r_1}(r_1), & R, r_1 \text{ plausible} \\ 0, & R, r_1 \text{ implausible,} \end{cases} \quad (23)$$

where $f_{r_a}(r_a)$ is uniform density function on the interval $[0, 0.2]$ (m), $f_R(R)$ is a uniform density function on the interval $[0, 1000]$ (m), $f_\Omega(\Omega)$ is a log-uniform density function on the interval $[0, 10^8]$ (s/m^2), and $f_{r_1}(r_1)$ is a uniform density function on the interval $[0, 1000]$ (m). Note that the leaky well, the injection well, and the observation well form a triangle with the sides of the triangle having length R , r_1 , and r_w . Due to geometric constraints, these three lengths cannot take arbitrary values (e.g., the length of one side cannot be greater than the sum of the lengths of the other sides). For R and r_1 to be plausible in equation (23), it must be possible that R , r_1 , and r_w be the lengths of the sides of a triangle.

3.3.1. Uncertainty in the Residual Distribution

In order to complete the description of how we deal with parametric uncertainty, we must specify the information-gap model for equation (5) which defines the discrepancies (residuals) between the model-predicted and observed pressures. We will utilize equation (6) where the mean, μ , is zero and the covariance of the observations within each screen is given by equation (20). The residuals in the upper observation screen are assumed to be independent of the residuals in the lower screen. The information-gap model will

treat H as uncertain with a nominal value of $H = 1/2$. This value of H corresponds to assuming that the residuals are an uncorrelated white noise. The information-gap model will then capture the possibility that the noise could be positively ($H > 1/2$) or negatively ($H < 1/2$) correlated.

Let $O_1^1, O_2^1, \dots, O_{30}^1$ denote the observations in the upper aquifer and $O_1^2, O_2^2, \dots, O_{30}^2$ denote the observations in the lower aquifer (see Figure 2). Define

$$f_H(\mathbf{O}|\mathbf{q}) = \prod_{i=1}^2 g_H(O_i^j - F_{30(i-1)+1}(\mathbf{q}), O_i^j - F_{30(i-1)+2}(\mathbf{q}), \dots, O_{30}^j - F_{30(i-1)+30}(\mathbf{q})), \quad (24)$$

where $g_H(\mathbf{x})$ is as given in equation (6) with the covariance function given in equation (20). This enables us to construct the information-gap uncertainty model of the residual distribution,

$$U(\epsilon) = \left\{ f_H(\mathbf{O}|\mathbf{q}) : \left| \frac{H - H_0}{H_0} \right| \leq \epsilon, H \in [0.2, 0.8] \right\}, \quad (25)$$

where $H_0 = 1/2$. The requirement that $H \in [0.2, 0.8]$ is to avoid numerical difficulties, and is not essential. However, it must be required that $H \in (0, 1)$ in any case. Note that $U(0) = \{f_{1/2}(\mathbf{O}|\mathbf{q})\}$ as required by equation (8). This states that the residuals are nominally a Gaussian white noise. Equation (7) is also satisfied by $U(\epsilon)$ for essentially the same reason that $M(\epsilon, \mathbf{q})$ satisfies equation (3).

3.4. Making a Decision

For this scenario, we supply two goals related to the physical behavior of the system. One states that the head increase in the upper aquifer observation screen due to the injection should be very small. This is desired in order to avoid hydraulic communication between the two aquifers, which could contaminate the upper aquifer. The other states that, due to the injection, the head increase in the lower aquifer observation screen should not be excessive, so as to avoid induced seismicity. Formally, these are expressed as

$$\max_{i=1,2,\dots,30} F_i < 7.5 \text{ (cm)}, \quad (26)$$

$$\max_{i=31,32,\dots,60} F_i < 10^3 \text{ (m)}, \quad (27)$$

resulting in the binary function

$$G(\mathbf{F}) = \begin{cases} 1, & \max_{i=1,2,\dots,30} F_i < 7.5 \text{ (cm)} \text{ and } \max_{i=31,32,\dots,60} F_i < 10^3 \text{ (m)} \\ 0, & \text{otherwise} \end{cases} \quad (28)$$

This makes it possible to apply equation (13). The results are presented in Figure 3. Site 2 has greater robustness for any value of P_0 , and would therefore be the site that is selected to do the large-scale CO_2 injection. In a case where the two curves cross, the decision maker would have to choose a value of P_0 (the maximum acceptable chance of failure), and the preferred site would be the one that has the greatest robustness at that value of P_0 . In this case, the potential for violating the first decision goal is ($\max_{i=1,2,\dots,30} F_i < 7.5 \text{ (cm)}$) is more restrictive than the more lenient second decision goal ($\max_{i=31,32,\dots,60} F_i < 10^3 \text{ (m)}$). Site 1 has lower resistivity, Ω (see Table 1), and this is what makes Site 1 less robust than Site 2.

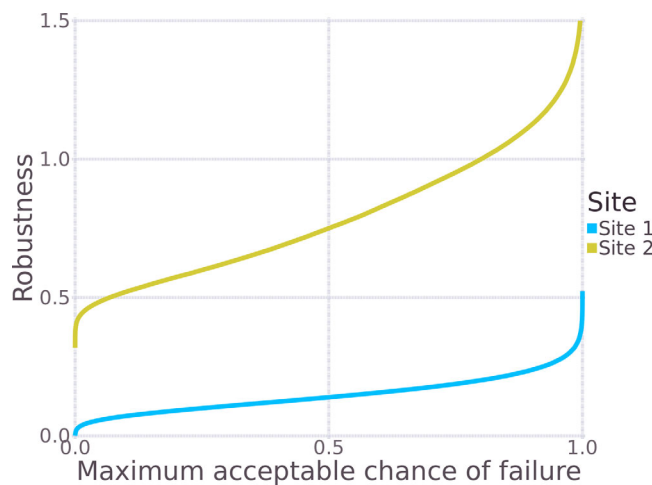


Figure 3. The robustness plotted against the maximum acceptable chance of failure, P_0 . Site 2 has greater robustness for any value of P_0 , and would therefore be the preferred site.

When the horizon of uncertainty is equal to zero, BIG DT reduces to

computing the probability of failure using Bayesian statistics. The Bayesian probability of failure is nearly zero for both sites considered here. This makes it hard to make a robust decision based on a purely Bayesian analysis, especially since there is significant uncertainty in the probability predicted by the Bayesian analysis (the error bars dominate the mean). The BIG DT approach, on the other hand, is able to demonstrate that Site 2 is more robust against uncertainty in the modeling and Bayesian analysis. Having full knowledge of the system, this robustness can be attributed to Site 1 having a leakier well than Site 2 (which is the only difference between the sites). Without full knowledge of the system, this is determined by considering the impact of uncertainty in the functional form of the physical model via the information-gap model in equation (21), and uncertainty in the Bayesian analysis via the information-gap model in equation (25).

With a Bayesian approach, we would seek to answer the question “What is the probability of failure?” Given that we do not know the conditional distribution functions needed to implement Bayes theorem correctly, the answer to this question that we would obtain would not be justified. Therefore, it would be imprudent to rely on this answer to make a critical decision. Instead, with the BIG DT approach, we seek to answer the question “How wrong can my assumptions be without the probability of failure exceeding a given threshold?” Decisions that allow the assumptions to be more wrong are considered to be more robust. It is in this sense that we say Site 2 is more robust against uncertainty than Site 1.

4. Conclusions

We have presented a general framework, called BIG DT, for making decisions in the presence of uncertainty. This framework combines Bayesian methods with information-gap decision theory, and makes it possible to incorporate part of the decision making process within the uncertainty quantification process. The design of the framework is motivated by earth science applications where severe uncertainties are frequently present and a representative set of outcomes cannot be enumerated in practice.

Demonstrating the general framework with a specific application, we explored a decision on site selection for geologic CO₂ sequestration. In this application, there were two decision goals that were considered. One sought to avoid induced seismicity in the host formation and the other sought to avoid contaminating an overlying aquifer. The product of this analysis (Figure 3) describes how wrong the modeling assumptions can be (the robustness) in terms of the amount of risk that the decision maker is willing to accept (the maximum acceptable chance of failure). For any level of risk, Site 2 allowed the modeling assumptions to be more wrong than Site 1 before exceeding this level of risk. Therefore, Site 2 was selected as the better site at which to sequester CO₂.

BIG DT provides a generalization of Bayesian methods to include nonprobabilistic uncertainty related to model inadequacy and the residual distributions used in Bayes theorem. The application we have considered here concerns geologic CO₂ sequestration, but can be applied much more broadly [see, e.g., O'Malley and Vesselinov, 2014b]. The approach was constructed with the intention of dealing with the severe uncertainties that are often found in subsurface and earth science applications.

Acknowledgments

This research was funded by the Environmental Programs Directorate of the Los Alamos National Laboratory; the Integrated Multifaceted Approach to Mathematics at the Interfaces of Data, Models, and Decisions (DiaMonD) project, Department of Energy, Office of Science; and an LANL Director's postdoctoral fellowship. The data used to produce the figures are available from the authors upon request.

References

- Avci, C. B. (1994), Evaluation of flow leakage through abandoned wells and boreholes, *Water Resour. Res.*, *30*(9), 2565–2578, doi:10.1029/94WR00952.
- Ben-Haim, Y. (2006), *Info-Gap Decision Theory: Decisions Under Severe Uncertainty*, 2nd ed., Academic, Oxford, U. K.
- Berger, J. O. (1985), *Statistical Decision Theory and Bayesian Analysis*, Springer, N. Y.
- Cihan, A., Q. Zhou, and J. T. Birkholzer (2011), Analytical solutions for pressure perturbation and fluid leakage through aquitards and wells in multilayered-aquifer systems, *Water Resour. Res.*, *47*, W10504, doi:10.1029/2011WR010721.
- Doughty, C., and K. Pruess (2004), Modeling supercritical carbon dioxide injection in heterogeneous porous media, *Vadose Zone J.*, *3*(3), 837–847.
- Gasda, S. E., S. Bachu, and M. A. Celia (2004), Spatial characterization of the location of potentially leaky wells penetrating a deep saline aquifer in a mature sedimentary basin, *Environ. Geol.*, *46*(6–7), 707–720.
- Gasda, S. E., J. Z. Wang, and M. A. Celia (2011), Analysis of in-situ wellbore integrity data for existing wells with long-term exposure to CO₂, *Energy Procedia*, *4*, 5406–5413.
- Gelfand, A. E., and A. F. Smith (1990), Sampling-based approaches to calculating marginal densities, *J. Am. Stat. Assoc.*, *85*(410), 398–409, doi:10.1080/01621459.1990.10476213.
- Geyer, C. J. (1992), Practical Markov chain Monte Carlo, *Stat. Sci.*, *7*, 473–483.
- Goodman, J., and J. Weare (2010), Ensemble samplers with affine invariance, *Commun. Appl. Math. Comput. Sci.*, *5*(1), 65–80, doi:10.2140/camcos.2010.5.65.

- Harp, D. R., and V. V. Vesselinov (2013), Contaminant remediation decision analysis using information gap theory, *Stochastic Environ. Res. Risk Assess.*, 27(1), 159–168, doi:10.1007/s00477-012-0573-1.
- Jewell, E. J., F. R. Abate, and E. McKean (2001), *The New Oxford American Dictionary*, vol. 6, Oxford Univ. Press, N. Y.
- Jung, Y., Q. Zhou, and J. T. Birkholzer (2012), Impact of data uncertainty on identifying leakage pathways in CO₂ geologic storage systems and estimating their hydrogeological properties by inverse modeling, in *TOUGH Symposium 2012*, Lawrence Berkeley National Laboratory, Berkeley, Calif.
- Jung, Y., Q. Zhou, and J. T. Birkholzer (2013), Early detection of brine and CO₂ leakage through abandoned wells using pressure and surface-deformation monitoring data: Concept and demonstration, *Adv. Water Resour.*, 62, 555–569.
- Lee, P. M. (2012), *Bayesian Statistics: An Introduction*, John Wiley, West Sussex, U. K.
- Liu, Y., H. Gupta, E. Springer, and T. Wagener (2008), Linking science with environmental decision making: Experiences from an integrated modeling approach to supporting sustainable water resources management, *Environ. Modell. Software*, 23(7), 846–858.
- Lunn, D., D. Spiegelhalter, A. Thomas, and N. Best (2009), The bugs project: Evolution, critique and future directions, *Stat. Med.*, 28(25), 3049–3067.
- Mandelbrot, B. B., and J. W. Van Ness (1968), Fractional Brownian motions, fractional noises and applications, *SIAM Rev.*, 10(4), 422–437, doi: 10.1137/1010093.
- Metropolis, N., A. W. Rosenbluth, M. N. Rosenbluth, A. H. Teller, and E. Teller (1953), Equation of state calculations by fast computing machines, *J. Chem. Phys.*, 21(6), 1087–1092, doi:10.1063/1.1699114.
- Metz, B., O. Davidson, H. De Coninck, M. Loos, and L. Meyer (2005), IPCC special report on carbon dioxide capture and storage, paper prepared by Working Group III of the Intergovernmental Panel on Climate Change (IPCC), Cambridge Univ. Press, Cambridge, U. K.
- Nogues, J. P., J. M. Nordbotten, and M. A. Celia (2011), Detecting leakage of brine or CO₂ through abandoned wells in a geological sequestration operation using pressure monitoring wells, *Energy Procedia*, 4, 3620–3627.
- Nordbotten, J. M., M. A. Celia, and S. Bachu (2004), Analytical solutions for leakage rates through abandoned wells, *Water Resour. Res.*, 40, W04204, doi:10.1029/2003WR002997.
- Nordbotten, J. M., M. A. Celia, S. Bachu, and H. K. Dahle (2005), Semianalytical solution for CO₂ leakage through an abandoned well, *Environ. Sci. Technol.*, 39(2), 602–611, doi:10.1021/es035338i.
- O'Malley, D., and V. Vesselinov (2014a), Groundwater remediation using the information gap decision theory, *Water Resour. Res.*, 50, 246–256, doi:10.1002/2013WR014718.
- O'Malley, D., and V. Vesselinov (2014b), A combined probabilistic/nonprobabilistic decision analysis for contaminant remediation, *SIAM/ASA J. Uncertain. Quantif.*, 2, 607–621, doi:10.1137/140965132.
- Plummer, M. (2003), JAGS: A program for analysis of Bayesian graphical models using Gibbs sampling, *Proceedings of the 3rd international workshop on distributed statistical computing*, vol. 124, Technische Universität Wien.
- Pruess, K. (2004), Numerical simulation of CO₂ leakage from a geologic disposal reservoir, including transitions from super- to subcritical conditions, and boiling of liquid CO₂, *SPE J.*, 9(02), 237–248.
- Stauffer, P., H. Viswanathan, R. J. Pawar, M. L. Klasky, and G. D. Guthrie (2006), CO₂-pens: A CO₂ sequestration systems model supporting risk-based decisions, in *Proceedings of the 16th International Conference on Computational Methods in Water Resources*, pp. 19–22, Technical University of Denmark, Copenhagen, Denmark.
- Stauffer, P. H., H. S. Viswanathan, R. J. Pawar, and G. D. Guthrie (2008), A system model for geologic sequestration of carbon dioxide, *Environ. Sci. Technol.*, 43(3), 565–570.
- Stehfest, H. (1970a), Algorithm 368: Numerical inversion of Laplace transforms [d5], *Commun. ACM*, 13(1), 47–49, doi:10.1145/361953.361969.
- Stehfest, H. (1970b), Remark on algorithm 368: Numerical inversion of Laplace transforms, *Commun. ACM*, 13(10), 624, doi:10.1145/355598.362787.
- Vihola, M. (2012), Robust adaptive metropolis algorithm with coerced acceptance rate, *Stat. Comput.*, 22(5), 997–1008, doi:10.1007/s11222-011-9269-5.
- Vrugt, J. A., C. Ter Braak, C. Diks, B. A. Robinson, J. M. Hyman, and D. Higdon (2009), Accelerating Markov chain Monte Carlo simulation by differential evolution with self-adaptive randomized subspace sampling, *Int. J. Nonlinear Sci. Numer. Simul.*, 10(3), 273–290, doi:10.1515/IJNSNS.2009.10.3.273.
- Wainwright, H. M., S. Finsterle, Y. Jung, Q. Zhou, and J. T. Birkholzer (2014), Making sense of global sensitivity analyses, *Comput. Geosci.*, 65, 84–94.
- Wang, R., and H.-J. Kumpel (2003), Poroelasticity: Efficient modeling of strongly coupled, slow deformation processes in a multilayered half-space, *Geophysics*, 68(2), 705–717, doi:10.1190/1.1567241.
- Wen, X.-H., and J. J. Gómez-Hernández (1996), Upscaling hydraulic conductivities in heterogeneous media: An overview, *J. Hydrol.*, 183(1), ix–xxxii.
- Zhou, Q., J. T. Birkholzer, and C.-F. Tsang (2009), A semi-analytical solution for large-scale injection-induced pressure perturbation and leakage in a laterally bounded aquifer-aquitard system, *Transp. Porous Media*, 78(1), 127–148.